Journal of Applied Polymer Science

Processing and Characterization of Supercritical CO_2 Batch Foamed Poly(lactic acid)/Poly(ethylene glycol) Scaffold for Tissue Engineering Application

Wenhao Zhang, Binyi Chen, Haibin Zhao, Peng Yu, Dajiong Fu, Jinsong Wen, Xiangfang Peng
The Key Laboratory of Polymer Processing Engineering of Ministry of Education, National Engineering Research Center of Novel Equipment for Polymer Processing, South China University of Technology, Guangzhou 510640, China
Correspondence to: X. Peng (E-mail: pmxfpeng@scut.edu.cn)

ABSTRACT: Both poly(lactic acid) (PLA) and poly(ethylene glycol) (PEG) are biodegradable polymers, blending PLA with PEG is expected to toughen PLA matrix while maintaining its biodegradability. In this study, PLA/PEG blends in different ratios were prepared through triple-screw extruder, and the foaming behavior was investigated using supercritical carbon dioxide as physical blowing agent. The mechanical, thermal, rheological properties, and crystallization behavior were also studied. By the incorporation of PEG, the impact strength of the PLA/PEG blends improved by 98% with the specimens fractured in a ductile mode. The crystallization process of the blends was accelerated, and the crystallinity was significantly increased to 45.1%. The viscoelasticity of the PLA/PEG matrix was weakened, and the cells tended to break at the cell wall during cell expansion; thus, a highly interconnected structure with a maximum porosity of 82.3% was obtained. Moreover, the PLA/PEG blends exhibited higher cell densities and smaller cell size, compared to their neat counterparts. © 2013 Wiley Periodicals, Inc. J. Appl. Polym. Sci. 130: 3066–3073, 2013

KEYWORDS: foams; biodegradable; blends; bioengineering; thermoplastics

Received 16 March 2013; accepted 9 May 2013; Published online 8 June 2013
DOI: 10.1002/app.39523

INTRODUCTION

Environmentally friendly polymers have attracted increasing interest in the past decades, which is an alternative to the exhaustion of petroleum resources. As a representative of this family, poly(lactic acid) (PLA) is not only biodegradable but also produced from renewable resources such as grain, corn, and molasses.[1,2] PLA is a linear aliphatic thermoplastic polyester that can be prepared either by condensation polymerization of the free acid or by catalytic ring opening polymerization of the lactide. PLA has excellent physical properties such as high strength, thermoplasticity, and processibility. Furthermore, it is biodegradable and biocompatible, because it can be naturally degraded in certain conditions. Because of these unique properties as well as its affordable cost when compared with other biodegradable polymers, PLA has been widely used in food packing, drug delivery, surgical repairment, and biological tissue-engineering scaffold fields.[3,4] However, its brittleness, low-heat deflection temperature, and poor barrier properties have significantly restricted its expansion into new areas. To overcome certain drawbacks while maintaining biodegradability, massive investigations have been conducted on the improvement of its ductility through plasticization, copolymerization, and blending with elastomers.[5–7]

The blending of polymers is an effective, practical, and economic way of obtaining materials with desirable properties.[8–10] Blending PLA with other polymers can substantially modify its mechanical and thermal properties, degradation rate, and permeability. PLA has been blended with elastomers such as LDPE, ABS, SEBS-MAH, PMMA, PC, ACR, EVA, MBS, EPDM, poly(-ethylene-*co*-octene) (EOR), and poly(ethylene-glycidyl methacrylate) (EGMA) to obtain a significantly improved ductility; however, the biodegradability and strength are universally weakened. The incorporation of PCL, PBS, PBSA, PBAT, TPS, PES, and PEG can enhance the ductility of PLA while maintaining its biodegradability. PLA/PCL blends have been extensively investigated, and various compatibilizers were used to improve the miscibility between PLA and PCL; the blend comprised a two-phase system with the PCL dispersed in the PLA matrix. Jin et al.[11] prepared PLA/PBAT blend with PBAT content vary from 5 to 20%; with the increase of PBAT content, the blends displayed decreased strength and modulus; however, elongation and toughness dramatically increased.

Poly(ethylene glycol) (PEG) is the polymers of ethylene oxide and is available in molecular weight ranging from 400 to 20000. PEG is known quite well for its nontoxic, biocompatible, and biodegradable property; in addition, the similar polarity of PEG

and PLA makes them miscible or partially miscible after melt blending. In view of its good properties, PEG is considered as a good candidate for improving the processing and properties of neat PLA and also the applications in tissue engineering scaffolds field (PLA and PEG were approved by the Food and Drug Administration for human clinical application). Hassouna et al.[12] developed PLA by grafting PEG via reactive extrusion, the *in situ* reactive grafting of PEG showed a clear effect on the thermal properties of PLA. Furthermore, Ren et al.[13] prepared magnetic PLA/PEG composite particles as carrier for drug-targeting delivery. Hu et al.[14] confirmed that large spherulites of PLA were formed followed by the crystallization of PEG on the edges; meanwhile, the amorphous phase underwent phase separation. Sheth et al.[15] showed that, below 50% PEG content, the tensile strength at yield significantly decreased with the increase in PEG content, while the elongation was improved. Park et al.[16] further prepared PLA and chain-extended PEG (CE-PEG) blends in an effort to toughen PLA without reducing tensile strength and modulus too much, the relative ductility of PLA/CE-PEG was 40 times higher than that of neat PLA.

For tissue-engineering applications, the role of the scaffold is to provide temporary support and direct the growth of the tissue; thus, a certain cell structure is necessary for the entrance of the cells and nutrient substance as well as the discharge of the metabolic waste. In general, an interconnected structure with controlled degradation rate, suitable mechanical sustainment, and surface chemistry properties is required.[17–19] Currently available techniques for fabricating polymer porous scaffold such as solvent casting, particulate leaching, electrostatic spinning, gas foaming, and phase separation[20,21] have developed with more or less success. Reignier et al.[22] prepared PCL scaffold using PEO and chloride salt particles as porogen, and the porosity of the scaffold can be controlled between 75 and 88% by altering the initial volume fraction of salt particals and changing the PCL/PEO composition ratio. Turng et al.[23] combined injection molding with supercritical fluids processing and particulate leaching to produce porous scaffold of PLA with the maximum porosity of 75%. Meanwhile, Ma and Zhang[24] produced PLLA scaffold material via phase-separation technique, and a porosity as high as 98.5% was achieved. However, the residual organic solvent in the scaffold can also represent an additional limitation of this method.

The combination of supercritical fluids technique and foaming is the most potential production method for its feasibility and nonbiological toxicity. Some research have been conducted to explore the foaming behavior of PLA, well-controlled cell structure of neat PLA, and PLA nanocomposites with cell size ranging from microscale (30 μm) to nanoscale (200 nm) were obtained, and the influence of foaming temperature and CO_2 pressure was further investigated.[25,26] However, few results associated with an ideal scaffold material were reported for lack of high porosity and connectivity between the cells,[27,28] and also the investigation of the foam behavior of PLA/PEG blend has not been reported so far.

The present work aims to enhance the ductility of PLA with PEG and investigates the effect of PEG on the morphology and foaming behavior as well as mechanical, thermal, and rheological properties of PLA/PEG blends. The overall goal was to produce PLA and PEG blends with suitable properties and idea cell structure while maintaining biodegradability.

EXPERIMENTAL

Materials

PLA (2002D, extrusion grade, M_w = 250,000 g/mol) with D-lactide content of 4% used in this work was purchased from Natureworks. PEG with a molecular of 6000 g/mol was purchased from Aoki Grease Industry Corporation. All materials were used as received. Carbon dioxide (purity, 99%) used as blowing agent was obtained from Shengtong Corporation.

Processing

PLA and PEG were predried in an oven for 4 h under 80 and 40°C, respectively. Blends of PLA and PEG at different ratios (100/0, 95/5, 90/10, and 80/20 by weight) were melt-blended via a triple-screw extruder at a constant rotor speed of 50 rpm, and the temperature profile from hopper to the die was set from 130 to 160°C. The mixtures were extruded using a four-strand die, naturally cooled, and pelletized. The pellets were hot-pressed at 190°C using a lab press and then quenched to room temperature to obtain PLA/PEG plates.

The foaming process was investigated by a homemade batch foaming device connected to a fluid pumping unit. Supercritical carbon dioxide was used as the physical foaming agent. The CO_2 pressure and temperature were controlled by the supercritical fluid pump and the thermocouple, respectively. Furthermore, a transducer was equipped with the autoclave to monitor the temperature and pressure during all the experiments. The sample introduced into the autoclave was cut from the compress-molded plates. The autoclave was heated to 160°C and pressurized with CO_2 at 20 MPa for 1 h in order to ensure sorption equilibrium of the entire sample. After sorption, the temperature was reduced to 90°C and instantaneously depressurized to atmospheric pressure to induce cell nucleation and growth. The solidification of the cell structure was realized through a water-cooling system.

Characterization

Mechanical Properties. The tensile testing of neat PLA and PLA/PEG blends was carried out in a universal test system (Instron5566, USA). For each test, the crosshead speed was 1 mm/min, and at least five samples were selected to guarantee the accuracy of the results. Izod impact tests were carried out on a POE200 (Instron Co, USA) pendulum impact testing machine using ISO standard specimens (80 × 10 × 4 mm, with a notch depth of 2 mm) machined from the compress-molded plates. The impact fracture surfaces should be kept properly in order to investigate the fracture morphology.

Differential Scanning Calorimetry. Differential scanning calorimetry (DSC) was carried out under nitrogen flow at a heating and cooling rate of 10°C/min to investigate the thermal properties of neat PLA and PLA/PEG blends with DSC204C (Netzsch, Germany). For each specimen, 8–10 mg was sliced from the extruded pellets and then crimp-sealed in aluminum crucibles. The samples were first heated from room temperature to 200°C and kept isothermal for 5 min to eliminate the heat

history, then cooled to −10°C, and subsequently scanned between −10 and 200°C.

Dynamic Mechanical Analysis. The influence of PEG on viscoelastic properties of PLA was analyzed by a dynamic mechanical analyzer (DMA). The rectangular samples were machined from the compress-molded plates with a specific dimension (50 × 10 × 4 mm). For this study, samples were heated from 20 to 100°C at a controllable rate of 3°C/min under flexural mode with a frequency of 1 Hz.

Polarized Optical Microscopy. A polarized light microscope (NESIS, Canada) with hot stage was used to observe the crystallization behavior of neat PLA and PLA/PEG blends. Samples were heated to 200°C on a glass slide for 3 min, then cooled to 120°C, and kept isothermal for a while.

Rheological Measurement. Rheological measurements of all the samples were performed on a Rheologic 5000 capillary rhemeter (CEAST Co, Italy) with a circular die. The diameter of the die was 1 mm, and *L*/*D* was 30:1. The measurements were conducted at 170°C, and the shear rate was 50, 100, 200, 500, 800, 1000, 1500, and 2000/s, respectively. Samples were compacted and preheated for 2 min in the barrel before the capillary experiments were started.

Scanning Electron Microscopy. Cell morphology and fracture surfaces from the impact tests were observed with the S-3700N (Hitachi, Japan) scanning electron microscopy operated at 10 kV. Foamed samples were immersed in liquid nitrogen for 30 min to maintain the cell structure and then fractured; all samples were sputter-coated with a thin layer of gold (−20 nm) before examination. The cell size and cell density were calculated using the Image-Pro Plus software, and the apparent density (ρ_{app}) of the foam samples was measured by pycnometer method. The porosity of the foam samples was determined by the following equation[29]:

$$V_f = \left(1 - \frac{\rho_{app}}{\rho_{PLA}}\right) \times 100\% \quad (1)$$

where V_f is the porosity of the sample and ρ_{PLA} is the density of the neat PLA, which is 1.31 g/cm^3.

RESULTS AND DISCUSSION

Mechanical Properties and Morphologies

Figure 1 presents the variation of tensile strength and impact strength as a function of PEG content, and the data are shown in Table I. Because of the brittle characteristic of PLA, the impact strength of neat PLA was 2.49 kJ/m^2. It is noticed that with the addition of 5 and 10% PEG, the impact strength of the PLA/PEG blend increased to 3.06 and 3.53 kJ/m^2, respectively. As the PEG content further increased to 20%, the impact strength of the blends continuously increased to 4.93 kJ/m^2, which was tremendously increased by 98% compared to that of neat PLA. It is expected that the presence of the low-molecular PEG enhanced the chain mobility of PLA; therefore, more impact energy can be absorbed by the PLA/PEG components. Accordingly, the elongation at break of the blends also improved

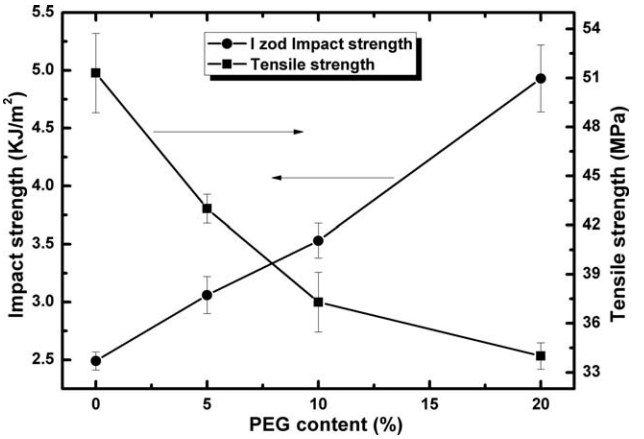

Figure 1. Tensile strength and impact strength with various PEG content.

with the increase in PEG content, and this is also attributed to the plasticization effect of PEG. However, the reduction of the tensile strength in this research was observed to be 16.2–33.7% as tradeoffs, which is consistent with the prior results obtained by Sheth[15] and Park.[16]

The impact fracture surface morphology (shown in Figure 2) was investigated to analyze the toughening mechanism of the PLA/PEG blends. Neat PLA [c.f. Figure 2(a)] exhibited a typical brittle fracture with a relatively smooth fracture surface. However, with the increase in PEG content, the impact fracture surface showed more evidences of ductile fracture as more and longer crack bridging and fibrils appeared. As shown in Figure 2(b), with the addition of 5% PEG, a certain degree of plastic deformation (e.g., ridges and crack bridging) emerged, and the surface became rougher. As the content of PEG further increased to 10 and 20%, the fracture surface changed significantly and large scale of plastic deformation (e.g., fibrils) was observed, and this was identified as an energy dissipation progress, which is in parallel with the impact test result. It is apparent that the addition of PEG imparts ductility to the PLA/PEG blends.

Thermal Properties

DSC heating traces of neat PLA and PLA/PEG blends were shown in Figure 3(a,b), and the numerical values were collected in Table II. The extra heat absorbed by the crystallites formed during heating was subtracted from the total endothermic heat flow caused by the melting of the total amount

Table I. Mechanical Properties of PLA/PEG Blends

PLA/PEG	Tensile strength (MPa)	Impact strength (KJ/m^2)	Elongation at break (%)
100/0	51.3 ± 2.4	2.49 ± 0.08	8.02
95/5	43.0 ± 0.9	3.06 ± 0.16	9.41
90/10	37.3 ± 1.8	3.53 ± 0.15	10.24
80/20	34.0 ± 0.8	4.93 ± 0.29	13.98

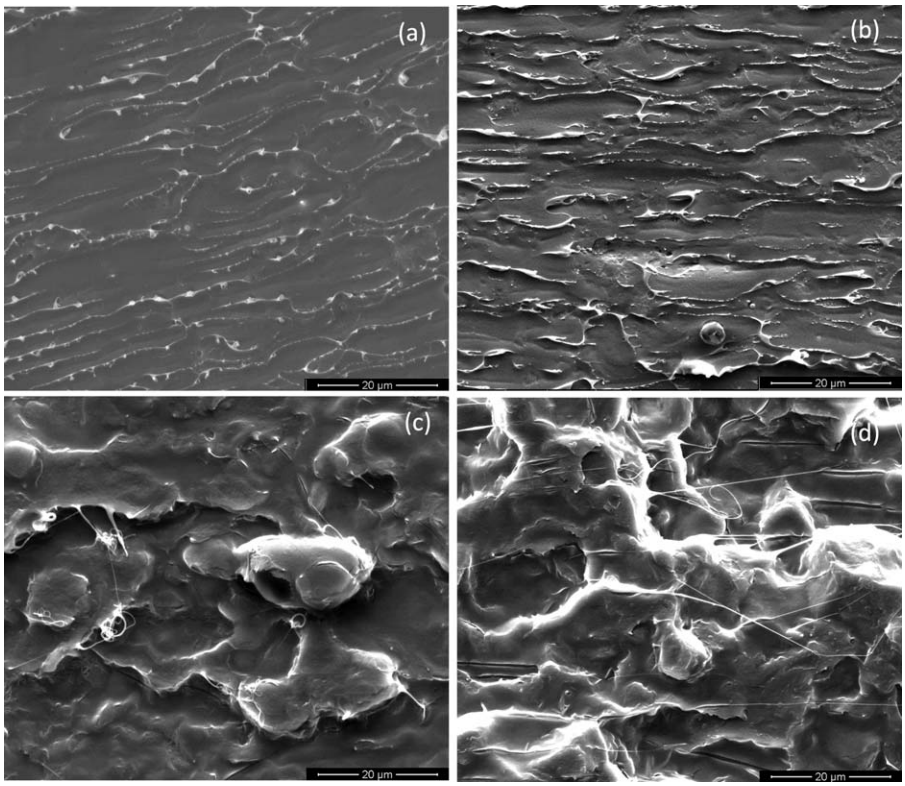

Figure 2. SEM micrographs of impact fracture surface of PLA/PEG blends. (a) Neat PLA, (b) PLA/PEG (95/5), (c) PLA/PEG(90/10), and (d) PLA/PEG (80/20).

of crystallites; thus, the crystallinity of PLA was calculated as follows:

$$\chi_c = \frac{\Delta H_m - \Delta H_{cc}}{\Delta H^0} \times \frac{100}{1 - \omega} \quad (2)$$

where ΔH_m is the enthalpy for melting, ΔH_{cc} is the cold-crystallization enthalpy, ΔH^0 is the enthalpy for a 100% crystalline PLA sample, which is 93.7 J/g, and ω is weight fraction of PEG in the sample.

During first heating [shown in Figure 3(a)], the glass transition of PLA/PEG blends shifted to lower temperature along with the increase in PEG content (from ~62 to 52.5°C). Furthermore, because the cooling rate was relatively fast during processing, no crystallization from the melt occurred for all the specimens, and the cold crystallization existed in the first heating. The incorporation of PEG significantly decreased the cold-crystallization temperature (from 107.3 to 80.4 °C) and narrowed peak width, which was resulted from the enhanced chain mobility and crystallization ability. During second heating [shown in Figure 3(b)], the glass transition of the PLA/PEG blends was diffused and can hardly detected by DSC method,[30] indicating that PLA and PEG were fully miscible after melt-blending. The cold-crystallization peak emerged for neat PLA while disappeared for the PLA/PEG blends, demonstrating that the incorporation of PEG accelerated the crystalline process, and the PLA/PEG blends reached the maximum crystallinity during the cooling process. Additionally, the melting point of the PLA/PEG blends slightly decreased compared to their neat counterparts. Because of the low nucleation and slow crystallization rate, neat PLA obtained a low degree of crystallization (4.3% in this study). However, the incorporation of PEG significantly improved the crystallinity of the blends to 45.1%, which was attributed to the increase in the crystalline rate and the reduction of the crystallization induction period. This is consistent with polarized optical results, which will be discussed below.

The temperature independence of storage modulus and loss tangent (tan δ) was measured by DMA, and the curves were displayed in Figure 4(a,b). In general, a declining trend of storage modulus for of the components was observed with a rapid reduction occurring at the glass transition region. At 20°C, the storage modulus of neat PLA was ~2.7 GPa, with the increase of PEG content, these values decreased to 2.6, 2.3, and 2.2 GPa, respectively. For neat PLA, the storage modulus fell abruptly within a narrow range at the onset of the glass transition (~50°C), whereas, for the PLA/PEG blends, the reduction occurred at a lower temperature over a broaden range (30–60°C for 5% PEG component), indicating that the presence of PEG significantly enhanced the chain mobility, and thus the transition to the rubber state could occur at lower temperature. Above the glassy region, the storage modulus of all the components tended to increase, which was attributed to cold-crystalization during heating. Furthermore, as the scanning rate was 3°C/min, the cold-crystalization occurred at a lower temperature compared to that identified by DSC (scanning rate was 10°C/min).

Applied Polymer SCIENCE

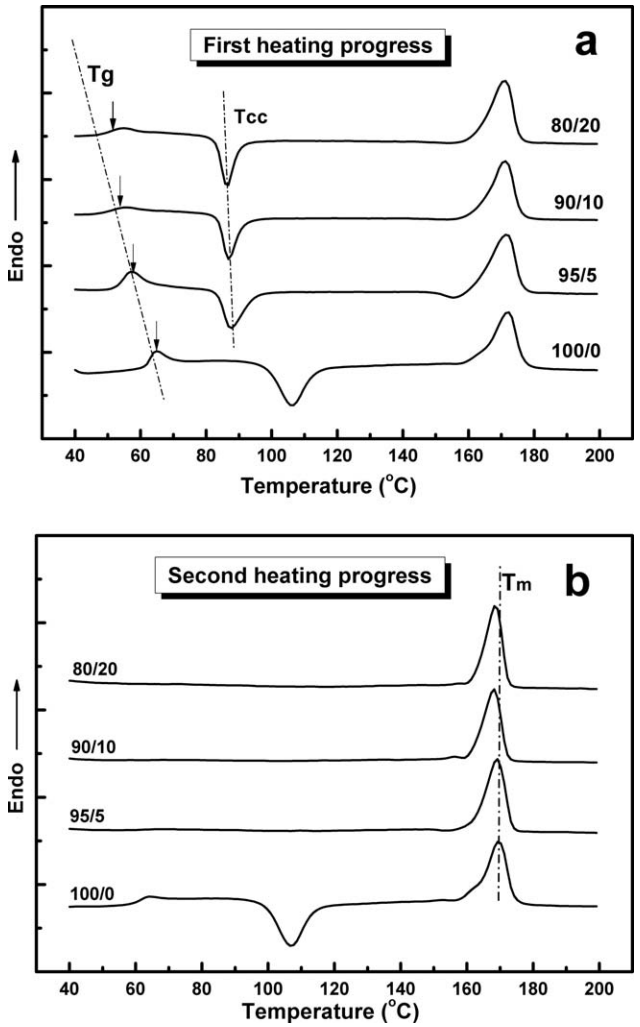

Figure 3. (a) First heating traces of PLA/PEG blends. (b) Second heating traces of PLA/PEG blends.

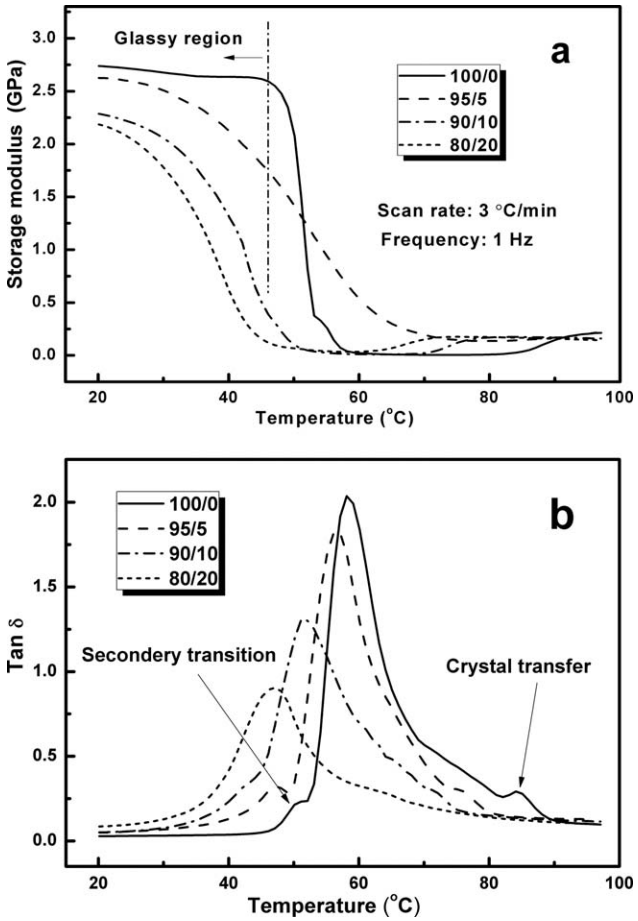

Figure 4. (a) Plots of storage modulus as a function of temperature. (b) Plots of loss tangent (tan δ) as a function of temperature.

Loss tangent (tan δ) is sensitive to the chain mobility, and the main transition peak is universally defined as the glass transition temperature. As shown in Figure 4(b), the glass transition temperature (T_g) of all the blends decreased with the increase of PEG content (from 58.1 to 47.1°C). For neat PLA and 5% PEG component, two shoulders appeared at each side of the main transition peak, which corresponded with the secondary transition and crystal transformation, respectively. As the PEG content increased to 10 and 20%, the chain mobility further enhanced and the shoulders disappeared.

Table II. Thermal Properties of PLA/PEG Blends

PLA/PEG	T_g (°C)[1]	T_{cc} (°C)	T_m (°C)	ΔH_{cc} (°C)[2]	ΔH_m (J/g)	χ_c (%)
100/0	61.3	107.3	170.3	−28.8	32.8	4.3
95/5	58.0	92.7	168.2	0	31.0	34.8
90/10	54.5	86.9	168.0	0	32.4	38.4
80/20	52.5	80.4	168.4	0	33.8	45.1

[a] T_g was obtained from the first heating; T_{cc} is the cold-crystallization temperature.
[b] ΔH_m and ΔH_{cc} were obtained from the second heating process.

Polarized Optical Microscopy

Polarized optical micrographs were obtained at the temperature of 120°C to further investigate the crystalline behavior of neat PLA and PLA/PEG blends. As shown in Figure 5, crystal morphology changed significantly by the presence of PEG. Figure 5(a) shows lager amounts of crystallites, which was closely associated with the fact that neat PLA has a relatively low-crystallization rate.[18] In Figure 5(b), the crystal size became larger; however, the crystallites still dominated, and only several isolated spherulites can be observed (as marked in the figure). Figure 5(c) shows integrated and clear spherulites with average size of 77 μm, demonstrating that the crystallization ability was enhanced by the presence of 10% PEG. Furthermore, it is notable to find that in Figure 5(d), the average crystal size increased to 131 μm as the PEG content further increased to 20%, the spherulites became crowded, and the spherulite boundary still maintains clear. It is apparent that the incorporation of PEG accelerated the growth process of the spherulites; thus, a relatively perfect crystalline structure was obtained, which is in accordance with the significantly increased crystallinity discussed in the previous part.

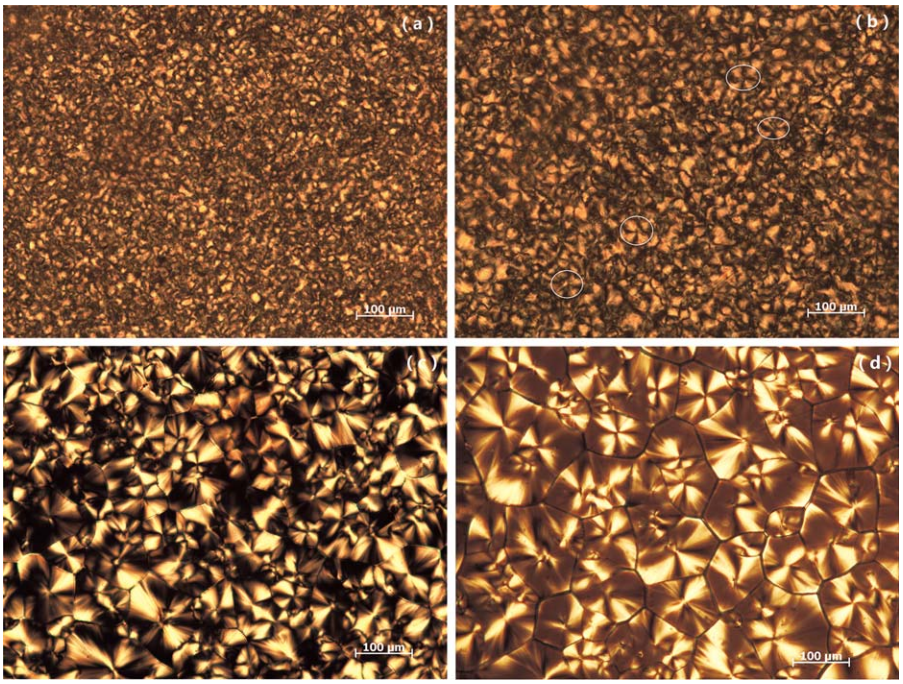

Figure 5. Polarization micrograph of PLA/PEG blends (200×). (a) neat PLA, (b) PLA/PEG (95/5), (c) PLA/PEG (90/10), and (d) PLA/PEG (80/20). [Color figure can be viewed in the online issue, which is available at wileyonlinelibrary.com.]

Rheological Measurement by Capillary Rhemeter

Figure 6 shows the curves of shear viscosity at different shear rates when the temperature was set at 170°C. It is noticed that both neat PLA and PLA/PEG blends exhibited strong shear-thinning behavior, indicating that the entanglement of polymer molecular chains unwrapped and orientated under shear stress. The addition of 5% PEG resulted in an obvious decrease in shear viscosity under lower shear rate compared to neat PLA; however, the difference became unconspicuous in higher shear rate region (above 1000 s^{-1}). As the PEG content further increased to 10 and 20%, the reduction of shear viscosity became larger. When the shear rate was 500 s^{-1}, the shear viscosity was 571, 487, 288, and 268 Pa s, respectively. That is to say, the addition of PEG increased the chain mobility and polymer free-volume; thus, a reduction of the shear viscosity of the blends was observed. During the foaming process, the cell nucleation and the following cell expansion are closely associated with the viscoelasticity of the matrix; as a result, the obtained rheological decrease is expected to have a significant effect on foaming with supercritical CO_2.

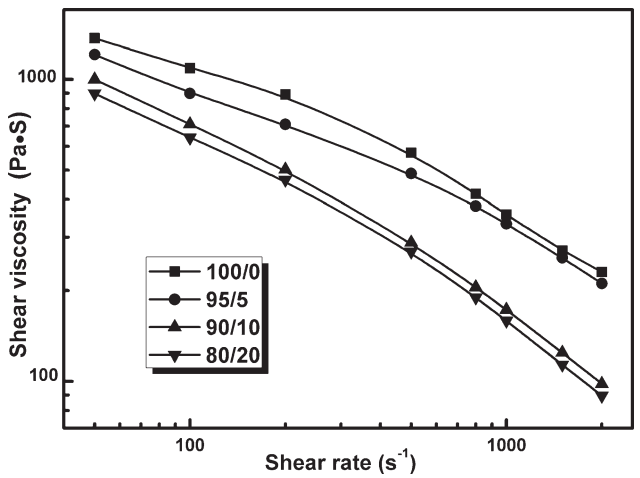

Figure 6. Variation of shear viscosity as a function of shear rate.

Foaming Behavior

For tissue-engineering scaffold applications, cell structure and porosity are important parameters, and they must match the type of tissue being regenerated[31]; thus, it is the key step to enhance the controllability of the cell structure. In this study, the foaming behavior of neat PLA and PLA/PEG blends was investigated by using a homemade foaming device. The SEM photographs shown in Figure 7 give an overview of the resulting cell morphologies. Neat PLA [c.f., Figure 7(a)] presented closed-cell structure, which was consistent with the prior results.[25,26] However, the PLA/PEG blends exhibited highly interconnected cell structure through the holes on the cell wall, and the bubbles with thinner cell wall became irregular. Besides, the connectivity of the cells enhanced with the increase in PEG content. Another feature that is noteworthy for the cell structure is that the opening gate between the cells was relatively big, which contributed to the propagation of the cells from one pore to another as well as the cell penetration from the scaffold surface to the internal. Additionally, a maximum porosity of 82.3% was obtained [calculated by eq. (1)], indicating that the addition of PEG enabled PLA to meet the requirements of tissue-engineering scaffold. As the foaming conditions such as time, temperature, and CO_2 pressure are similar, the cell expansion mainly depends on the viscoelastic properties of the matrix. According to the aforementioned rheological

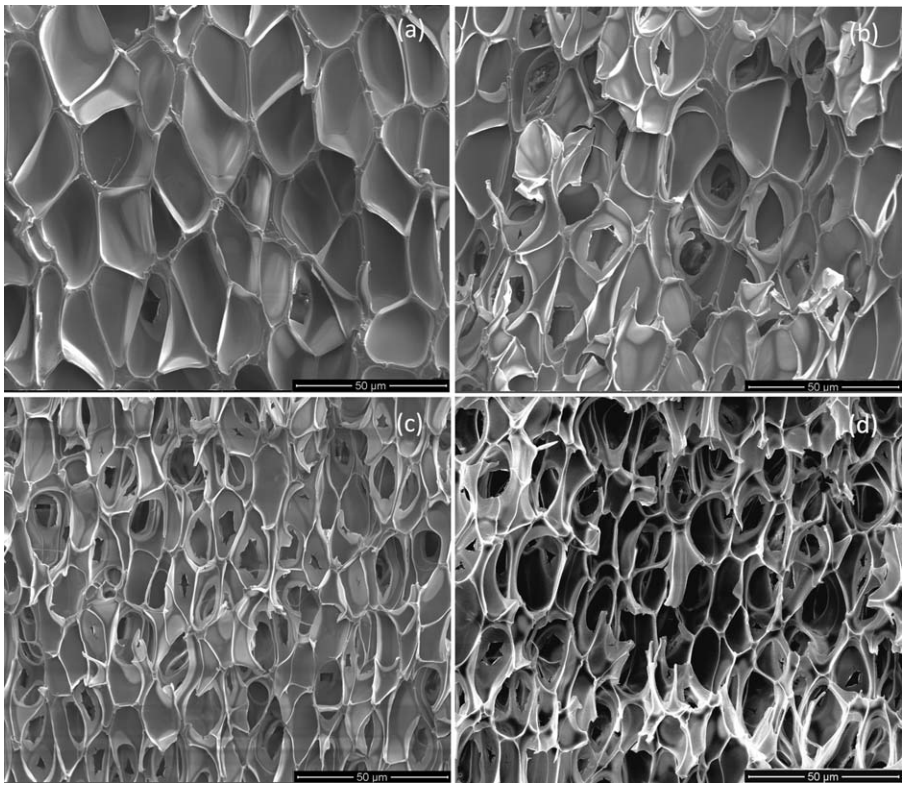

Figure 7. SEM micrographs of cell morphology. (a) neat PLA, (b) PLA/PEG(95/5), (c) PLA/PEG(90/10), and (d) PLA/PEG(80/20).

measurement results (shown in Figure 6), the incorporation of PEG reduced the viscosity of the matrix; besides, the elasticity of matrix was also weakened by the CO_2-induced plasticization effect; thus, the matrix became too weak to sustain the cell expansion, and the cells had a tendency to break at the cell wall, which resulted in a highly porosity and interconnected structure.

As a semicrystalline polymer, the foam behavior of PLA is complex due to the presence of the highly ordered crystalline structure. For one thing, the small molecular (e.g., CO_2) is unable to diffuse into the crystalline region. For another, the crystalline domains may serve as heterogeneous nucleation sites, and the nucleation can also occur at the interface of the crystalline regions and the amorphous regions. What is more, the developed crystalline structure makes the matrix stiffer, and the cell expansion process is hindered.[21,32,33] Mihai et al.[34] investigated the crystallinity development in the foamed PLA using supercritical carbon dioxide as the physical blowing agent, and it was shown that the crystalline structure enhanced the cell-formation process. Liao et al.[35] found that, during foaming process, the presence of CO_2 induced the crystallization of PLA, which had a great influence on the final cell morphology.

As shown in Figure 7, the PLA/PEG blends exhibited smaller cell size and higher cell density compared to their neat counterparts. Because of the interconnected cell structure of the PLA/PEG blends, an important gas loss occurred during cell expansion, thus leading to a reduced cell size.[36] Furthermore, the inhibitional effect of crystallization on cell expansion confirmed by Jenkins et al.[21] may also contribute to the reduced cell size. The crystalline structure developed in the matrix served as heterogeneous nucleation sites, and this nucleation enhancement resulted in the higher cell densities of the PLA/PEG blends. In view of the cell-size distribution of the PLA/PEG blends, it has been confirmed to be a suitable size for the growth of the bone fibers (10–40 μm) as well as the cultivation of the human osteoblast cells *in vitro* (5–50 μm).[37–39]

CONCLUSIONS

To increase the ductility of PLA, a series of PLA/PEG blends were prepared using a triple-screw extruder. By the addition of PEG, the impact strength and elongation at break of the blends increased while the tensile strength decreased to some extent; moreover, the failure mode changed from brittle fracture of neat PLA to ductile fracture of the blends. The crystallization process of PLA/PEG blends was accelerated, and the spherulite size became larger. A noteworthy feature for the cell structure is that the bubbles of the PLA/PEG blends tended to break at the cell wall during cell expansion, which was due to the incorporation of PEG and the CO_2-induced plasticization effect. Furthermore, the connectivity between the bubbles enhanced with the increase in PEG content. The PLA/PEG blends exhibited higher cell densities and smaller cell size compared to their neat counterparts, which was attributed to the heterogeneous nucleation effect of the crystal structure of PLA. Moreover, a desirable porosity of 82.3% was obtained, demonstrating that the PLA/PEG composite was a suitable tissue-engineering scaffold material.

ACKNOWLEDGMENTS

The authors acknowledge the financial support of the National Natural Science Foundation of China (No.51073061, No.21174044), the Nature Science Foundation of Guangdong Province in China (No.9151064000010), the Fundamental Research Funds for the Central Universities (No.2011ZZ0011) and 973 Program (2012CB025902).

REFERENCES

1. Liao, X.; Nawaby, A. V.; Naguib, H. E. J. *Appl. Polym. Sci.* **2012**, *124*, 585.
2. Li, H. B.; Huneault, M. A. *Polymer* **2007**, *48*, 6855.
3. Bleach, N. C.; Nazhat, S. N.; Tanner, K. E. P. *Biomaterials* **2002**, *23*, 1579.
4. Turnan, D.; Sirin, H.; Ozkoc, G. J. *Appl. Polym. Sci.* **2011**, *121*, 1067.
5. Wu, X. H.; Ghzaoui, A. E.; Li, S. M. J. *Am. Chem. Soc.* **2011**, *27*, 8000.
6. Lee, H.; Park, J. B.; Chang, J. Y. J. *Polym. Sci., Part A: Polym. Chem.* **2011**, *49*, 2859.
7. Dorati, R.; Genta, I. *Polym. Degrad. Stab.* **2007**, *92*, 1660.
8. Ge, H. H.; Yang, F.; Hao, Y. P.; Wu, G. F.; Zhang, H. L.; Dong, L. S. J. *Appl. Polym. Sci.* **2013**, *127*, 2832.
9. Park, J. W.; Im, S. S.; Kim, S. H.; Kim, Y. H. *Polym. Eng. Sci.* **2000**, *40*, 2539.
10. Li, G.; Sarazin, P.; Orts, W. J.; Imam, S. H.; Favis, B. D. *Macromol. Chem. Phys.* **2011**, *212*, 1147.
11. Jin, S. Q.; Xia, H.; Liang, Y. R. *New Chem. Mater.* **2007**, *35*, 60.
12. Hassouna, F.; Raquez, M. J.; Addiego, F.; Dobois, P.; Toniazzo, V.; Ruch, D. Eur. *Polym. J.* **2011**, *47*, 2134.
13. Ren, J.; Hong, H. Y.; Ren, T. B.; Teng, X. R. *Mater. Lett.* **2005**, *59*, 2655.
14. Hu, Y.; Hu, Y. S.; Topolkaraev, V.; Hiltner, A.; Baer, E. *Polymer* **2003**, *44*, 5681.
15. Sheth, M.; Kumar, R. A.; Dave, V.; Gross, R. A.; Mccarthy, S. P. J. *Appl. Polym. Sci.* **1997**, *66*, 1495.
16. Park, B. S.; Song, J. C.; Park, D. H.; Yoon, K. B. J. *Appl. Polym. Sci.* **2012**, *123*, 2360.
17. Kozlowski, M.; Masirek, R.; Gazicki-Lipman, M. J. *Appl. Polym. Sci.* **2007**, *105*, 269.
18. Li, H. B.; Huneault, M. A. *Polymer* **2007**, *48*, 6855.
19. Zhong, R.; Wang, H. K.; Na, B. J. *Kunming Univ. Sci. Technol.* **2010**, *35*, 18.
20. Kohlhoff, D.; Ohshima, M. *Macromol. Mater. Eng.* **2011**, *296*, 770.
21. Jenkins, M. J.; Harrison, K. L.; Silva, M. M. C. G.; Whitaker, M. J.; Shakesheff, K. M.; Howdle, S. M. *Eur. Polym. J.* **2006**, *42*, 3145.
22. Reignier, J.; Huneault, M. A. *Polymer* **2006**, *47*, 4703.
23. Kramschuster, A.; Turng, L. S. J. *Biomed. Mater. Res., Part B: Appl. Biomater.* **2010**, *92*, 366.
24. Ma, P. X.; Zhang, R. J. *Biomed. Mater. Res.* **1999**, *46*, 60.
25. Fujimoto, Y.; Ray, S. S.; Okamoto, M.; Ogami, A.; Yamada, K.; Ueda, K. Macromol. *Rapid. Commun.* **2003**, *24*, 457.
26. Ema, Y.; Ikeya, M.; Okamoto, M. *Polymer* **2006**, *47*, 5350.
27. Pilla, S.; Kramschuster, A.; Yang, L. Q.; Lee, J.; Gong, S. Q.; Turng, L. S. *Mater. Sci. Eng. C.* **2009**, *29*, 1258.
28. Seo, J. H.; Han, J. *Polym. Plast. Technol.* **2012**, *51*, 455.
29. Jain, S.; Reddy, M. M. *Mater. Eng.* **2010**, *295*, 750.
30. Kozlowski, M.; Masirek, R.; Gazicki-Lipman, M. J. *Appl. Polym. Sci.* **2007**, *105*, 269.
31. Coombes, S. C.; Rizzi, A. G. A.; Williamson, M.; Barrralet, J. E.; Downes, S.; Wallace, W. A. *Biomaterials* **2004**, *25*, 315.
32. Hedenqvist, M.; Gedde, U. W. *Prog. Polym. Sci.* **1996**, *21*, 299.
33. Baldwin, D. F.; Park, C. B.; Suh, N. P. *Polym. Eng. Sci.* **1996**, *36*, 1446.
34. Mihai, M.; Huneault, M. A.; Favis, B. D. J. *Appl. Polym. Sci.* **2009**, *113*, 2920.
35. Liao, X.; Nawaby, A. V.; Whitfield, P. S. *Polym. Mint.* **2010**, *59*, 1709.
36. Corre, Y. M.; Maazouz, A.; Duchet, J.; Reignier, J. J. *Supercrit. Flu.* **2011**, *58*, 177.
37. Stevens, M. M.; George, J. H. J. *Science* **2005**, *310*, 1135.
38. Karageorgiou, V.; Kaplan, D. J. *Biomater.* **2005**, *26*, 5474.
39. Akav, G.; Birch, M. A.; Bokhari, M. A. J. *Biomater.* **2004**, *25*, 2577.